JAST, Vol. 2, No. 4, pp 1–8

JAST
Journal of Aerospace Science and Technology

Experimental Studies of Inverted-Profile Coaxial Jet Flows

P. Behrouzi[1], J.J. McGuirk[2]

A generic single coaxial jet model was designed, constructed, and tested in a water tunnel specially designed for STOVL (Short Take Off and Vertical Landing Aircraft) flow applications. Laser Doppler Anemometry (LDA) surveys and Laser Induced Florescence (LIF) image capture were used to visualize the global flow patterns and identify the mean velocity and turbulence structure of an inverted-profile coaxial impinging jet, with and without a crossflow. Effects of the outer/inner jet velocity ratio and vertical jet/ horizontal crossflow velocity ratio on the development of the coaxial jet flow field were studied. The results presented are suitable for CFD validation purposes.

NOMENCLATURE

D_i	Internal diameter of inner nozzle of co-axial system
D_o	Internal diameter of outer annular nozzle of co-axial system
LDA	Laser Doppler Anemometry
LIF	Laser Induced Fluorescence
W_o	Outer bulk mean velocity at nozzle exit
W_i	Inner bulk mean velocity at nozzle exit
$w - rms$	rms of W velocity fluctuations
W	Time-average vertical velocity
U	Time-average axial velocity
U_c	Crossflow mean velocity
x	Axial direction
y	Spanwise direction
z	Vertical direction

INTRODUCTION

The multiple lift jets associated with a short take-off/vertical landing (STOVL) aircraft (Figure 1) in its near-ground hovering or landing phase of flight create a complex three-dimensional flowfield confined between the airframe surface and the ground plane. This flowfield contains several identifiable sub-components or basic fluid flow types, e.g., multiple jet impingement, ground vortex flow, fountain up-wash flow, etc. The interaction of these flows influences the flow around the aircraft, as well as introducing complex design and operational problems such as hot gas ingestion, aircraft-suck-down and jet-induced lift forces which can, for example, cause difficulty in controlling aircraft pitching moment variations. For the design and development of new STOVL aircraft configurations, it is essential to understand fully the implications of these aerodynamic interactions caused by ground effects. A wind or water tunnel capability for the study of ground effect flows is desirable and often used for both preliminary design studies and subsequent configuration development. As reported by Jones et al [1], NASA has established a large database for supersonic and subsonic jets exhausting into a subsonic flow field. Bray [2] has reviewed experimental studies of single and multiple jet impingement. The water tunnel study of Saripalli [3] for impinging jet flows provided the first fundamental and detailed fluid mechanics data on fountain flow phenomena as influenced by parameters such as jet pitch spacing. Barata et al. [4] have included crossflow effects, but considered only the case of twin and three-poster vertical jets. Stewart & Kuhn's [5] tests provided a detailed examination of the flowfield generated in ground effect. However, detailed measurements of the flow properties in the impingement zone and in the fountain upwash associated with multiple jet impingement are scarce and have been

1. *Dept. of Aeronautical and Automotive Eng., Loughborough Univ., Loughborough, Leicestershire, LE11 3TU, UK; Email: P.Behrouzi@lboro.ac.uk.*
2. *Dept. of Aeronautical and Automotive Eng., Loughborough Univ., Loughborough, Leicestershire, LE11 3TU, UK; Email: J.J.McGuirk@lboro.ac.uk.*

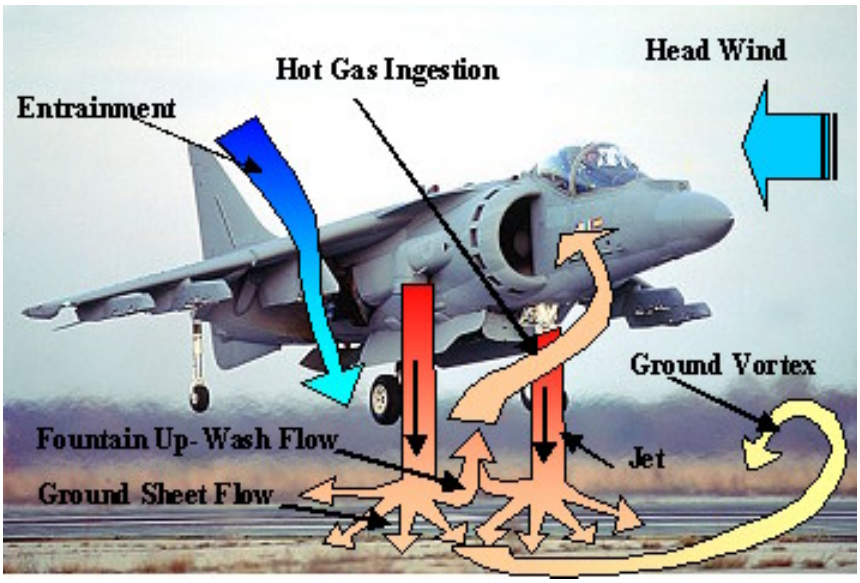

Figure 1. Major aerodynamic features associated with STOVL aircraft in ground effect.

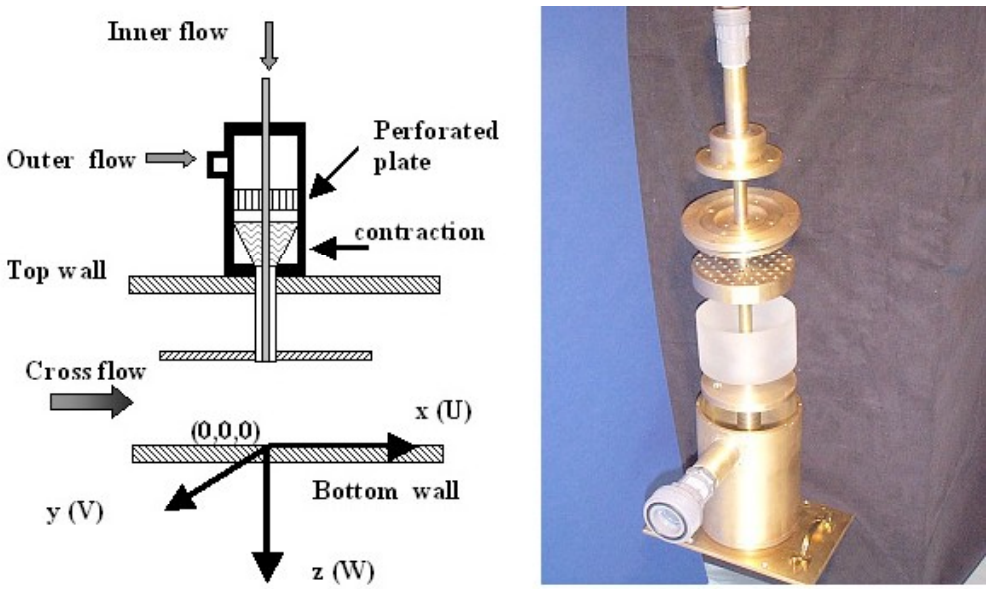

Figure 2. Schematic and photo of the coaxial jet assembly

essentially presented only in the absence of crossflow and with the use of pneumatic probe instrumentation. Saripalli [3] did report on the turbulence properties of the flow and observed very high turbulence levels and spreading rates in the fountain. Although the basic flow mechanisms that combine to produce the ground effect flow patterns beneath STOVL aircraft are known, details of these mechanisms are still not adequately understood. In particular, the effect of the velocity profile shape at nozzle exit has received little attention to date. Interest in the effect of jet exit velocity profile shape on ground effect flow patterns has recently increased due to proposals for future STOVL aircraft configurations which involve a separate, forward-mounted lift engine (either shaft or gas driven). The exhaust from such a lift engine might have a noteable profile variation due, for example, to the presence of a hot, low velocity core flow and a cooler high-speed outer annular fan flow. As part of a programme to produce CFD validation data for a range of impinging jet and ground effect flows, many jet impingement configurations have been designed and studied (Behoruzi and McGuirk [6 to 12]). This prior work has focused on fountain upwash flow and the ground vortex region in order to quantify the aerodynamic mechanics which control the hot gas ingestion phenomenon. All the data in

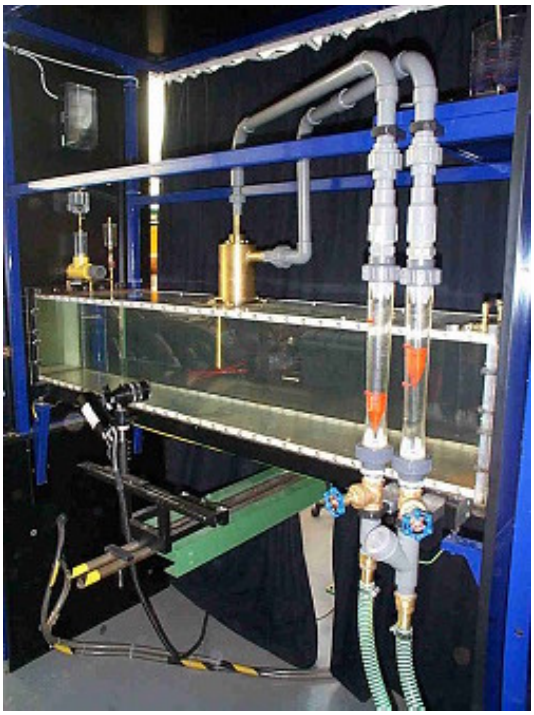

Figure 3. Water Tunnel test section and the coaxial nozzle unit set-up

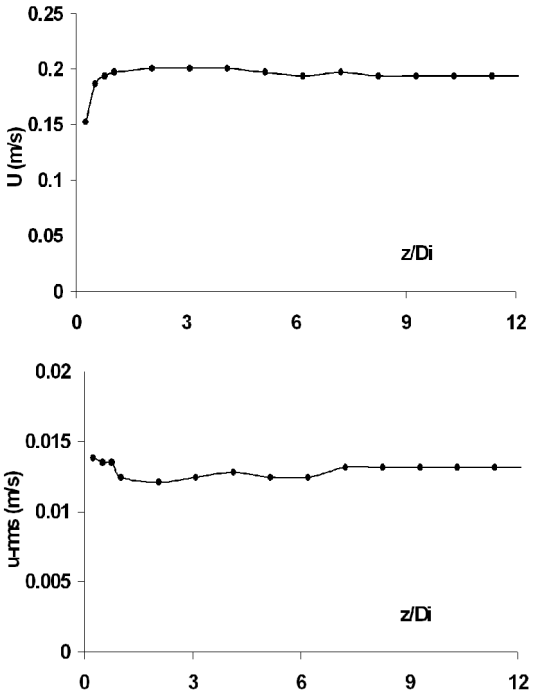

Figure 4. Mean and rms of crossflow axial velocity profiles near the jet unit.

Refs. [6-12] were taken for the simplest jet velocity profile at nozzle exit, namely an essentially flat profile with thin nozzle wall boundary layers. In reality, as described above, the nozzle exit profile may assume a more complex form, and may even, for example,

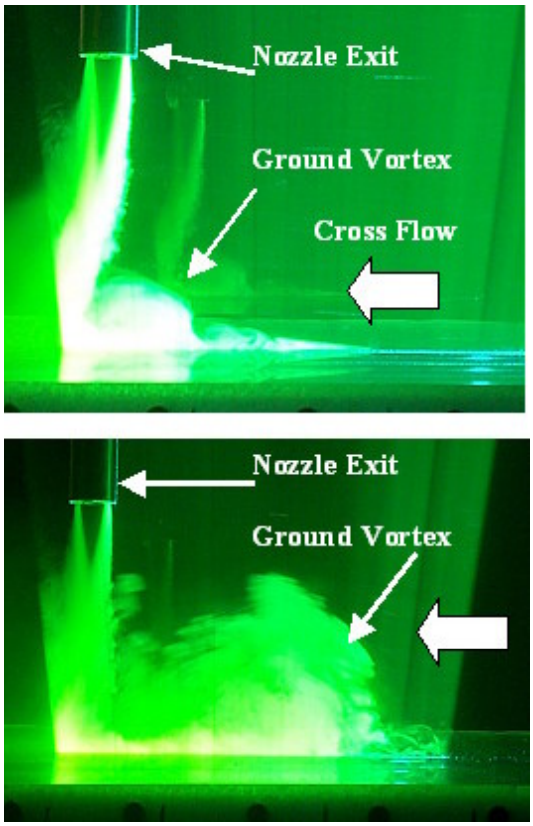

Figure 5. LIF photos of the coaxial nozzle symmetry plane showing size and location of the ground vortex under two flow conditions of W_o/W_i=1.5(top) and W_o/W_i=3(bottom).

correspond to a nozzle exit flow made up of a central round jet surrounded by an annular jet of different velocity (here referred to as a 'co-axial' jet profile). The present study was therefore aimed at extending the work reported in Refs. [6-12] to consideration of nozzle exit velocity profile shape. In particular, the velocity of the outer annular stream is assumed to be greater than the velocity of the inner round core jet leading to a so-called 'inverted' profile co-axial jet. The implication of the presence of such a coaxial jet profile at nozzle exit for a descending STOVL aircraft could drastically change aerodynamic, acoustic and ground erosion characteristics of the impinging jet. However, the information on co-axial jet impingement is very scarce. Kirkham and Knowles [13] have published some data but, since only pneumatic probes were used, this provided no turbulence information and did not investigate the impingement zone in any detail or include crossflow effects. Both free jet (no ground plane) and impinging jet cases (ground plane heights of 2,4,10 inner jet diameters) were measured. Velocity profile information for a range of outer/inner jet nozzle pressure ratios were considered, corresponding to a range of outer/inner jet velocity ratios from around 1.2 to 1.9, with data concentrated mainly in the free

jet region (jet decay rate/spreading rate) or in the developed wall jet region (wall jet decay) well away from impingement. In addition, because there is a substantial and growing interest in jet noise reduction, and the inverted profile shape has some benefits here, Ko and Kwan [14] studied the initial region of subsonic coaxial jets at three different outer/inner velocity ratios including the inverted shape. Their results suggested that noise reduction was related to the dynamics of two categories of vortices at different frequencies. The higher-frequency or primary vortices were found to be generated in the inner jet/outer jet mixing region, and the lower frequency or secondary ones in the outer jet/ambient flow mixing region. Their growth or decay and their dominance depended strongly on the outer/inner mean-velocity ratio.

In the present work the database on co-axial jet impingement with an inverted profile shape at nozzle exit is extended. A generic coaxial-jet unit was designed and constructed for use in an existing water-tunnel facility. Non-intrusive Laser Doppler Anometery (LDA) was used to gather mean and turbulence data on the flowfield for a range of conditions. Laser Induced Fluorescence (LIF) was employed to visualize the jet flow patterns.

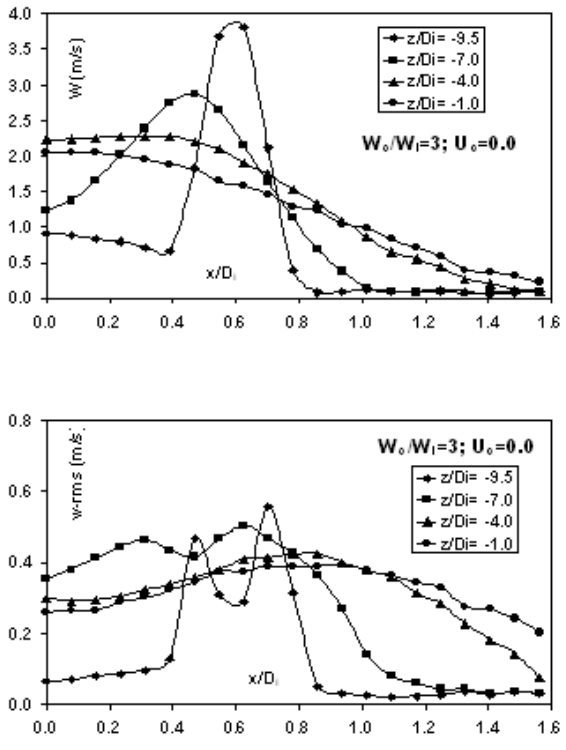

Figure 6. Measured mean and rms of vertical velocity (W); x-direction profiles on coaxial jet symmetry plane at different heights above the ground plane.

THE EXPERIMENTAL FACILITY

The experiments were conducted in a specially designed and constructed water tunnel for impinging jet flow problems, which has previously been described in detail by Behrouzi & McGuirk [6]. The main advantage of a water facility over conventional wind tunnels is that it provides a convenient means to perform flow visualisation. Because of the lower kinematic viscosity of water compared to air, it is possible to reproduce a flow at a given Reynolds number with a lower characteristic velocity in a water tunnel than a wind tunnel for the same length scale (a velocity reduction by around a factor of 15). Due to the smaller velocity scale, the flow time scales are relatively longer, leading to easier and clearer observation and capture of dynamic phenomena. The rig is of re-circulating design. The test section dimensions are 1.125m long, 0.37m wide and 0.3m high. The test section is made of Perspex (Plexiglas) to allow ample optical access for both LDA and flow visualisation measurements from both side and top/bottom orientations. Two flow circuits are provided, namely a horizontal crossflow circuit and a vertical jet flow circuit. Pumps extract water from a main supply tank and pump it to a large settling chamber on the upstream end of the test section (for crossflow) or to jet header tanks above the test section which feed inner and outer coaxial jet units. A flow quality and turbulence management system is provided in the crossflow circuit to provide controlled and well-defined conditions at inlet to the test section. The turbulence management system represents a fairly standard combination of a contraction section, perforated plates, honeycomb and coarse- and fine-mesh screens and has been demonstrated to provide uniform and low turbulence level crossflow through the test section in tests conducted in the present tunnel and reported by Behrouzi and McGuirk [6].

Figure 2 presents a schematic and a photo of the coaxial jet unit. Figure 3 illustrates the water tunnel with the coaxial nozzle unit on top of the test section. This unit is positioned centrally in the test section and is supported by the test section top-wall. The ID and OD diameters of the inner axisymmetric nozzle, outer annular nozzle are 12.8/13.4 mm and 19.4/25.4 mm respectively. The coaxial nozzle impingement height above the test section tunnel floor height is 128 mm. The diameter and area ratios (outer/inner) of the coaxial nozzle are therefore 1.52 and 1.2 respectively, and the impingement height h/D_i is 10. These dimensions are close to parameters used in other published papers in this field.

Laser Doppler Anemometry (LDA) is the most suitable choice for the point-wise measurement of components of both mean and fluctuating velocity in complex, highly turbulent 3D flows. This type

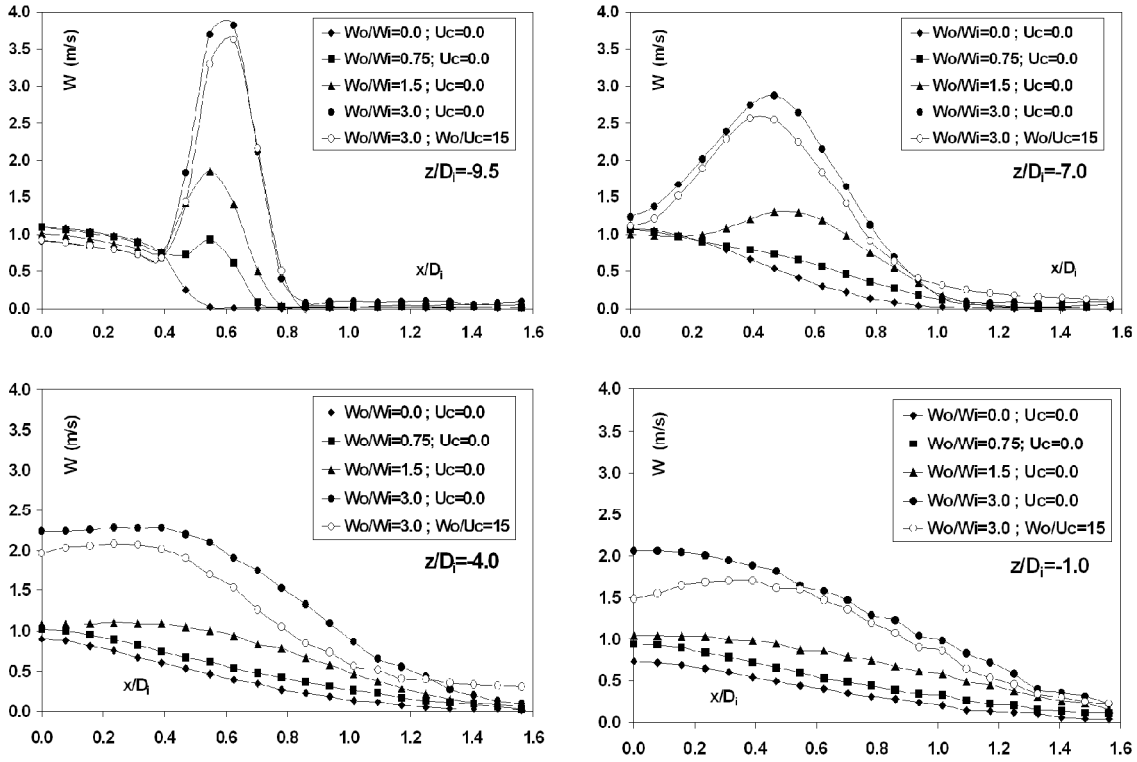

Figure 7. Measured mean vertical velocity (W);x-direction profiles on coaxial jet symmetry plane at two heights, at different inner/outer velocity ratios, and with and without crossflow.

of measurement employs the phenomenon of Doppler shifting of incident light frequency to measure the velocity of small particles (of order 1 micron) suspended in the fluid. The attraction of this method is that, being a purely optical method, it does not interfere with or perturb the flow in any way since no measuring probes have to be introduced. An inexpensive, robust and commonly used system is a single-channel one operating in forward-scatter fringe mode, and this is employed in the present investigation. The resulting scattered light signals captured by the photo-multiplier were processed using a TSI IFA 550 processor connected to a PC and controlled by a ZECH LDA data acquisition interface (model 1400A). No corrections were made for the sampling bias, any associated errors were minimized by using high data rates compared to typical velocity fluctuation rates, as suggested by Erdmann and Tropea [15]. The signal processor was operated in the trigger mode so that the data were acquired at fixed time intervals; a typical sampling rate used was 2KHz.

EXPERIMENTAL PROCEDURE

Preliminary experiments were performed using the LDA system (to provide inlet boundary condition data for CFD studies) and to check the quality of the mean velocity and turbulence intensity of the coaxial jet and the crossflow where these entered the test section. Mean and turbulence levels at the inner and outer coaxial jet exit planes can be extracted from the graphs presented in Figs 8 and 9 at the height of z/D_i=-9.5 (the closet possible line of measurement). Crossflow mean and rms axial velocity profiles approaching the coaxial jet unit are presented in Figure 4.

The accuracy and repeatability of the data taken in the flow field depended on the sampling time, especially in regions where the flow was highly turbulent. More accurate data are obtained where a larger number of independent samples are collected to form the mean values, but this will clearly increase the measurement time per point. The effect of all LDA system settings such as sample number, data rate, trigger mode, frequency shift, etc. on the repeatability of the measurements was studied. To minimize statistical (random) errors, the number of individual velocity samples used in the experiments to form time-mean averages was set at 20,000 (sampling time 10 seconds) for all data points. This was not necessary in all regions of the flow, but was found essential for meaningful averages in, for example, the fountain and ground vortex zones. Three flow conditions were chosen for data gathering. These progressively introduced flow complexity in terms of co-axial jet velocity ratio and

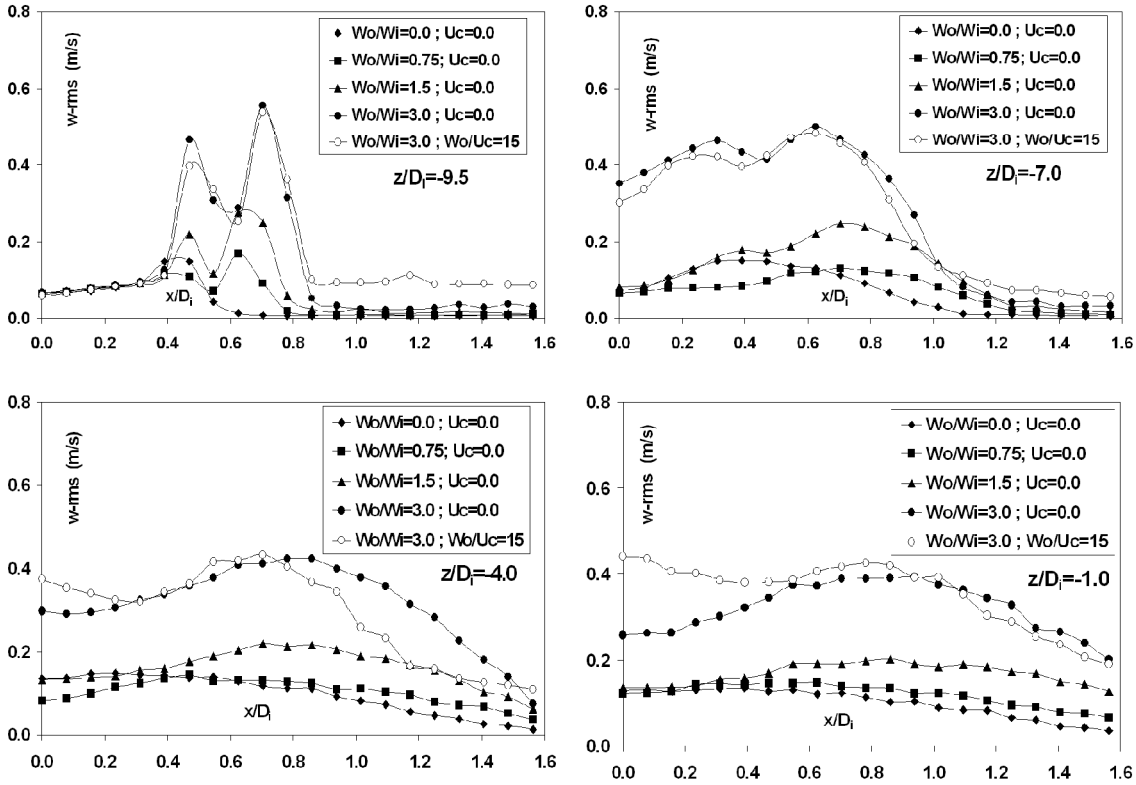

Figure 8. Measured rms vertical velocity (w-rms);x-direction profiles on coaxial jet symmetry plane at two heights, at different inner/outer velocity ratios, and with and without crossflow.

crossflow velocity ratio (n.b: here W_o, W_i and U_c are nozzle exit outer velocity, inner velocity, and crossflow velocity respectively):

- Test case-1: no crossflow and no outer flow ; W_o =0.0: W_i =1 m/s; U_c =0; effectively a single round impinging jet experiment.
- Test case-2: no crossflow but three outer flow velocities of W_o =0.75, 1.5 and 3 m/s ,: with W_i =1 m/s (velocity ratios 0.75, 1.5 and 3); to capture outer/inner flow interaction and effects on impingement.
- Test case-3: as test case-2 but with crossflow of U_c =0.2 m/s (outer jet/crossflow velocity ratios of 3.75, 7.5 and 15) ; to capture the effect of crossflow and introduce a ground vortex.

The outer/inner and outer/crossflow velocity ratios studied are similar to, but extend the range covered by Kirkham and Ko [13].

In the co-ordinate system used below to report the measurements (See Figure 2), the longitudinal x co-ordinate (i.e. in the crossflow or headwind direction) is positive in the crossflow direction, the vertical z co-ordinate is positive downwards, and finally the spanwise y co-ordinate is positive towards the front of the rig to form a right-handed co-ordinate system. The origin of the co-ordinates is at the geometrical jet impingement point on the ground plane.

RESULTS AND DISCUSSIONS

Laser Induced Fluorescence (LIF) was used initially for flow visualisation to establish the flow structure. The beam from a 5 Watt CW Argon-Ion laser was converted to a light sheet by a cylindrical lens. The sheet passed into the flow region of interest entering through the water tunnel floor. Fluorescent dye was added to the outer jet flow, and the laser sheet caused the dye to fluorescence. The emitted light was captured by a camera viewing normal to the light sheet through the tunnel front wall. Figure 5 presents visualisations of the coaxial jet impingement region for two different outer flow velocities of 1.5 and 3 m/s and in the presence of a 0.2 m/s crossflow, i.e. velocity ratios of the coaxial jet (outer/inner) of 1.5 and 3.0, and outer jet/crossflow velocity ratios of 7.5 and 15. The effect of the outer jet flow momentum on the development of the impinging jet and its associated ground vortex is considerable. Since dye was added just to the outer jet, the outer/inner jet mixing and inner jet potential core length are clearly visualised;

the core length roughly halves as the outer jet velocity is increased. The weaker outer/inner velocity ratio (top photo) bends over more in the crossflow as expected, leading to a weaker impingement, although even at this impingement height (h/D_i=10) a small ground vortex is still observed. The stronger impingement with the higher outer/inner velocity ratio (bottom picture) leads to a more vertical jet trajectory and a much larger ground vortex, penetrating twice as far into the crossflow and rising to about half the impingement height.

Figure 6 presents x-direction profiles of LDA measured mean and rms vertical velocity on the coaxial jet symmetry plane at four different heights for the highest velocity ratio and zero crossflow. At the nearest plane

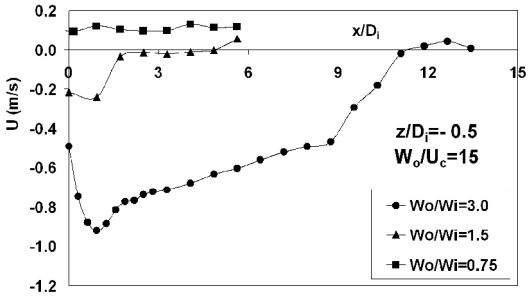

Figure 9. Measurement of x-direction mean velocity near ground plane for coaxial jet, capture of ground vortex behavior.

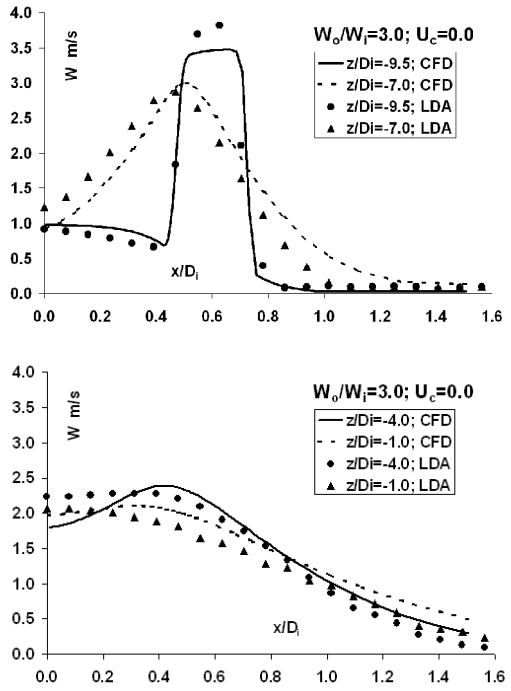

Figure 10. CFD prediction of the inverted-profile coaxial flow (outer/inner velocity ratio of 3.0).

to jet discharge (z/D_i=-9.5) the inverted shape of the co-axial jet velocity profile can be clearly recognized. The peak velocity moves towards the nozzle centerline and the inner jet has been completely entrained by the outer by z/D_i=-1 ($9D_i$ from jet discharge), a slight peak is still just visible at z/D_i=-4. The jet velocity then starts to decelerate as the ground impingement plane is approached. Turbulence generation in the shear layers surrounding the annular jet is clearly visible, with the turbulence level slightly higher in the outer shear layer (~30% turbulence intensity) since the strain rate is higher there than on the inner side with no ambient flow. The double peaked shape is still visible at z/D_i=-7.0, but changes for the other two profiles measured are closer to the ground plane, although the peak turbulence level is still found in the outer annular jet shear layer. The turbulence level will start to increase as impingement occurs, but this has not started to happen at the last measurement plane at $1D_i$ above the ground floor.

Figures 7 and 8 present the effects of varying the outer/inner velocity ratio as well as the introduction of a crossflow on the coaxial jet development for the same 4 heights used in Figure 6. Outer/inner velocity ratios of 0, 0.75, 1.5 and 3 were studied. The effect of the crossflow has been captured for the outer/inner velocity ratio of 3 only. For the time-averaged vertical velocity (Figure 7), with no crossflow, the transition from an inverted profile shape to a "normal" jet shape (with the peak velocity at the jet centreline), obviously occurs more rapidly as the outer/inner velocity ratio decreases. For example, the inverted shape has already disappeared for W_o/W_i = 1.5 at z/D_i = -4, whereas for W_o/W_i = 3.0 an outboard peak is just still visible. For outer/inner velocity ratios less than 1.0, a normal jet shape is established very quickly (at z/D_i = -7). The effect of the crossflow was examined for W_o/W_i = 3.0. The change in the jet trajectory and the increase in the crossflowing entrainment both lead to lower vertical velocity at all heights in the presence of crossflow. For the turbulence field (w-rms, Fig 8), reduced outer/inner velocity ratio implies lower levels of strain rate and, hence lower turbulence levels. The effect of crossflow immediately after jet discharge (z/D_i = -9.5, -7) is relatively small, but the change in the jet trajectory causes 3D effects so that the flow is no longer symmetrical about the $x/D_i = 0$ plane, and this is first seen over in the turbulence profiles at the two lower heights measured even though the mean velocity profiles appear quite symmetric.

Figure 9 presents measurements which capture ground vortex characteristics. The ground vortex only occurs with crossflow, so only W_o/U_c = 15 data are presented, but for a range of W_o/W_i. The measured data represent the axial (x-direction) mean velocity component along an x-direction profile upstream of

the impingement point and close to the ground surface (z/D_i = -0.5). The negative U velocity region identifies the ground vortex size. At the largest co-axial jet vertical momentum condition (W_o/W_i = 3.0), the ground vortex streches to more than 10 D_i upstream. As W_o/W_i reduces, the ground vortex size shrinks rapidly so that at W_o/W_i = 0.75 no ground vortex can be identified at all.

As an illustration of the use of the present measurements for CFD validation purposes, a structured 3D, pressure-based code (Reference [16]) was applied to the present flow problem. An eddy viscosity closure (two-equation k-ϵ model) was used as the turbulence model. Curvilinear grid systems fitted to both the coaxial jet exit geometry and the water tunnel geometry were generated. Preliminary predictions of the flow for an outer/inner velocity ratio of 3 (no crossflow) are presented in Figure 10. The trend of the prediction is very close to experimental results with the transition from an inverted shape profile to a normal jet shape near the ground floor well captured.

SUMMARY

A generic vertically impinging coaxial jet model was constructed and tested in a specially designed water tunnel for STOVL flow applications. Laser Doppler Anemometry (LDA) was employed to measure the mean velocity and turbulence levels of the flowfield. Tests were performed for three outer/inner velocity ratios and one vertical jet/horizontal crossflow velocity ratio. The outer/inner co-axial jet ratio mainly influenced the transition distance in the vertical jet from an inverted profile shape to a normal jet profile. The higher outer/ inner velocity ratios displayed the expected behaviour of stronger impingement and a larger ground vortex zone. Profiles of time-averaged velocity and turbulence normal stress were measured at several vertical heights, and captured the changing flow type from jet like to impingement flow. The data presented can also serve as validation data for time-averaged turbulence-model-based RANS CFD predictions, and one demonstration of this kind was provided.

REFERENCES

1. Jones, A.L., Flood, J.D., Amuedo, K.C., Strock, T.W., "Hot Gas Ingestion Testing of an Advanced STOVL Concept in the NASA Lewis 9- by 15-Foot Low Speed Wind Tunnel With Flow Visualisation", *AIAA-88-3025*, (1988).
2. Bray, D., "Jets in Crossflow and Ground Effect", Ph.D. Thesis, Cranfield Institute of Technology(1992).
3. Saripalli, K.R. , "Laser Doppler Velocimetry Measurements in 3D Impinging Twin-Jet Fountain Flows", *Turbulent Shear Flows*, Edited by Durst et al., Springer-Verlag, Berlin, **5**, PP 147-168(1987).
4. Barata, J.M.M., Durao, D.F.G., and Heitor, M.V., "Laser Doppler Measurements of Multiple Impinging Jets Through a Crossflow", *4th Int. Symposium on Applications of Laser Anemometry in Fluid Mechanics*, Lisbon, Portugal, (1988).
5. Stewart, V.R., and Kuhn, R.E., "Characteristics of the Ground Vortex Developed by Various V/STOL Jets at Forward Speed", *AIAA-83-2494*, (1983).
6. Behrouzi, P & McGuirk, J.J., "Experimental Data for CFD Validation of Impinging Jets in Crossflow with Application to ASTOVL Flow Problems", AGARD Conference Proceedings 534, Computational and Experimental Assessment of Jets in Crossflow, Winchester, PP 8.1-8.11(1983).
7. Behrouzi, P. and McGuirk, J.J., "Experimental Data for Validation of the Intake Ingestion Process in STOVL Aircraft", *Journal of Flow Turbulence and Combustion*, PP 233-251(2000).
8. Behrouzi, P. and McGuirk, J.J., "Twin-Jet Impingement Flow Survey Data for CFD Validation of STOVL Flows", *Canadian Aeronautics and Space Journal*, **45**(4), PP 350-357(1999).
9. Behrouzi, P. and McGuirk, J.J., "Laser Doppler Velocimetry Measurements of Twin-Jet Impingement Flow Validation of Computational Models", *Optic and Lasers in Engineering Journal*, **30**, PP 265-277(1998).
10. Behrouzi, P., "LDA Experimental Data for CFD Validation of a Three-Poster Jet Impingement System", *AERO 2000 Proceeding*, First International & Third Bi-Annual Conference of the Iranian Aerospace Society, Tehran, Iran, **4**, PP 39-51(2000).
11. Behrouzi, P. and McGuirk, J.J, "Particle Image Velocimetry for Intake Ingestion in Short Take-off and Landing Aircraft", *AIAA Journal of Aircraft* , **37(6)**, PP 994-1000(2000).
12. Page, G.J., McGuirk, J.J., Behrouzi, P., Hossain, M. and Fisher, M.J., "A CFD Coupled Acoustics Approach for the Prediction of Coaxial Jet Noise", *Proceedings of NATO RTO-AVT Symposium*, Part A - Developments in Aero- and Hydro-Acoustics, Manchester, UK, PP 1-10(2001).
13. Kirkham L. and K. Knowles, "Inverted Profile Coaxial Jet Flows Relevant to ASTOVL Applications", *The Aeronautical Journal*, **102**, PP 377-384(1998).
14. Ko, N.W.M. and Kwan, A.S.H., "Initial Region of Subsonic Co-Axial Jets", *J. Fluid Mech*, **73**, PP 305-332(1976).
15. Erdmann, J.C., and Tropea, C.D., "Turbulence-Induced Statistical Bias in Laser Anemometery", *Proc. of 7th Biennial Symposium of Turbulence*, Rolla, USA, (1981).
16. Page, G.J., Zhao, H., and McGuirk J.J., "A Parallel Multiblock Reynolds Averaged Navier-Stokes Method for Propulsion Installation Applications", *Paper 16.4*, 12th ISABE Conference, Melbourne, Australia, (1995).